

Ab initio study of compressed Ar(H₂)₂: Structural stability and anomalous meltingClaudio Cazorla^{1,*} and Daniel Errandonea²¹*Department of Chemistry, University College London, London WC1H 0AJ, United Kingdom*²*Departamento de Física Aplicada, ICMUV, Fundació General Universitat de Valencia, Valencia, Spain*

(Received 24 February 2010; published 16 March 2010)

We study the structural stability and dynamical properties of Ar(H₂)₂ under pressure using first-principles and *ab initio* molecular-dynamics techniques. At low temperatures, Ar(H₂)₂ is found to stabilize in the cubic C15 Laves structure (MgCu₂) and not in the hexagonal C14 Laves structure (MgZn₂) as it has been assumed previously. Based on enthalpy energy and phonon calculations, we propose a temperature-induced MgCu₂ → MgZn₂ phase transition that may rationalize the existing discrepancies between the sets of Raman and infrared vibron measurements. Our AIMD simulations suggest that the melting line of Ar(H₂)₂ presents negative slope in the interval $60 \leq P \leq 110$ GPa. We explain the origin of this intriguing physical phenomenon in terms of decoupling of the Ar and H₂ degrees of freedom and effective thermal-like excitations arising from coexisting liquid H₂ and solid Ar phases.

DOI: [10.1103/PhysRevB.81.104108](https://doi.org/10.1103/PhysRevB.81.104108)

PACS number(s): 64.70.dj, 81.30.-t

I. INTRODUCTION

Solid hydrogen H₂ is expected to become metallic at compressions higher than 400 GPa.¹ In fact, experimental signatures of the long-sought insulator-to-metal phase transition remain elusive up to pressures of ~ 340 GPa.² Accepted pressure-induced mechanisms by which the metallicity of hydrogen can be enhanced involve atomization of H₂ molecules and partial filling of electronic σ_u^* molecular levels due to charge transfer from or band hybridization with other chemical species.³⁻⁵ Already in the earlier 90s Loubeyre *et al.*,³ based on the disappearance of the Raman (R) vibron mode and the darkening of the material, claimed to observe metallization of the Ar(H₂)₂ compound when compressed in the diamond anvil cell (DAC) up to ~ 200 GPa. The stable room-temperature (RT) phase structure of this compound was identified with the hexagonal C14 Laves structure typified by the MgZn₂ crystal (space group: *P63/mmc*). Strikingly, posterior synchrotron infrared (IR) measurements did not show evidence of molecular bonding instabilities nor metallic Drude-type behavior up to at least 220 GPa.⁶ Subsequently, Bernard *et al.*⁷ suggested that activation of H₂ dissociation processes and corresponding development of metallization in Ar(H₂)₂ could occur via a solid-solid phase transition of the MgZn₂ → AlB₂ (space group: *P63/mmc*) type at pressures already within the reach of DAC capabilities. However, recent *ab initio* work done by Matsumoto and Nagara⁸ demonstrates that the onset of metallicity in the AlB₂ structure commences at pressures significantly higher than in pure bulk H₂.

In view of the growing interest on hydrogen-rich van der Waals (vdW) compounds under pressure,^{4,9} partly motivated by the hydrogen-storage problem, and of the unresolved discrepancies described above, we have conducted a theoretical study on Ar(H₂)₂ under extreme *P-T* conditions using first-principles density-functional theory calculations and *ab initio* molecular-dynamics simulations (AIMD). In this paper, we present results showing that at low temperatures and pressures up to ~ 215 GPa the Ar(H₂)₂ crystal stabilizes in the cubic C15 Laves structure typified by the MgCu₂ solid

(space group: *Fd3m*). This structure has not been considered in previous works^{7,8,10} though its probable relevance to Ar(H₂)₂ was pointed out recently.¹¹ On the light of first-principles enthalpy and phonon calculations, we propose a temperature-induced (pressure-induced) phase transition of the MgCu₂ → MgZn₂ (MgZn₂ → MgCu₂) type that may clarify the origin of the discrepancies between the sets of R and IR data. Furthermore, in the high-*P* regime ($P \sim 210$ GPa) we find that a metallic hydrogen-rich liquid can be stabilized at temperatures of ~ 4000 K wherein H-H coordination features render molecular dissociation activity. By means of AIMD simulations, we estimated an upper bound of the melting curve $P(T_m)$ of Ar(H₂)₂ and found a negative $\partial T_m / \partial P$ slope spanning over the interval $60 \leq P \leq 110$ GPa. Our simulations show that the lattice composed by H₂ molecules melts at temperatures significantly lower than the lattice of Ar atoms does, so leading to stable mixtures of coexisting liquid H₂ and solid Ar over wide *P-T* ranges. We propose an argument based on this atypical physical behavior to explain the cause of the estimated negative $\partial T_m / \partial P$ slope.

II. OVERVIEW OF THE CALCULATIONS

Our calculations were performed using the all-electron projector augmented wave method and generalized gradient approximation of Wang and Perdew as implemented in the VASP code.¹² Dense Monkhorst-Pack special *k*-point meshes¹³ for sampling of the first Brillouin zone (IBZ) and a cut-off energy of 400 eV were employed to guarantee convergence of the total energy per particle to within 0.5 meV. In particular, we used $8 \times 8 \times 8$, $8 \times 8 \times 4$, and $12 \times 12 \times 12$ *k*-point grids for calculations on the perfect unit cell corresponding to the MgCu₂, MgZn₂, and AlB₂ crystal structures, respectively. All the considered crystal structures were relaxed using a conjugate-gradient algorithm and imposing the forces on the particles to be less than 0.005 eV/Å. The phonon frequencies in our calculations were obtained using the small-displacement method^{14,15} over the unit cells (Γ -point phonon frequencies) and large supercells containing 80 at-

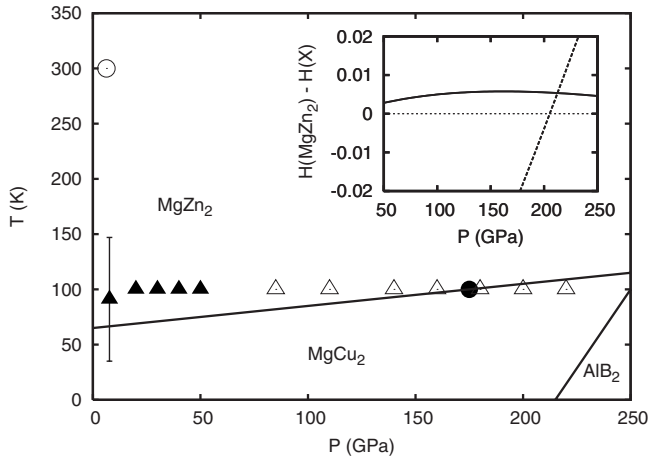


FIG. 1. Schematic low- T phase diagram of $\text{Ar}(\text{H}_2)_2$ under pressure. MgZn_2 - MgCu_2 and MgCu_2 - AlB_2 phase boundaries are sketched according to the results and arguments presented in the text. Thermodynamic states at which x-ray, R and IR vibron measurements were carried out are indicated (Ref. 3): x-ray= \circ , (Ref. 3) R= \bullet , (Ref. 17) IR= \blacktriangle , and (Ref. 6) IR= \triangle . Inset: enthalpy difference per particle of the MgCu_2 (solid line) and AlB_2 (dashed line) structures with respect to the MgZn_2 Laves phase as function of pressure at zero temperature.

oms. *Ab initio* molecular-dynamics simulations were carried out in the canonical ensemble (N, V, T) using bulk supercells of $\text{Ar}(\text{H}_2)_2$ containing 160 atoms (Γ -point sampling). At given pressure, the dynamical properties of the system were sampled at 400 K intervals from zero temperature up to the melting curve of pure Ar. Temperatures were maintained using Nosé-Hoover thermostats. A typical AIMD simulation consisted of 3 ps of thermalization followed by 7 ps over which statistical averages were taken. It is worth noticing that we recently used a very similar computational approach to the one described here to study the energetic and structural properties of $\text{Ar}(\text{He})_2$ and $\text{Ne}(\text{He})_2$ crystals under pressure,¹¹ and that very recent experiments¹⁶ have confirmed the validity of our predicted $P(V)$ curves.

III. RESULTS AND DISCUSSION

A. Low- T results

A series of candidate structures were considered in our *ab initio* enthalpy $H(P)$ calculations (rutile, fluorite, MgNi_2 , etc.), however, only the MgZn_2 , MgCu_2 , and AlB_2 structures turned out to be energetically competitive so the following analysis concentrates on these ones. Ignoring quantum zero-point motion effects, we found that $\text{Ar}(\text{H}_2)_2$ is energetically more stable in the MgCu_2 structure than in either the MgZn_2 or AlB_2 structures at pressures $P \leq 215$ GPa (see Fig. 1). Also we predicted that at $P_t = 215(1)$ GPa the solid transitions from the MgCu_2 to the AlB_2 structure. The calculated zero-temperature equation of state of $\text{Ar}(\text{H}_2)_2$ in the MgCu_2 structure displays very good agreement with respect to the available experimental data⁷ (see Fig. 2). For instance, at $V = 14.61$ and $12.50 \text{ \AA}^3/\text{particle}$ we obtain a pressure of 8.83 GPa and 17.14 GPa, respectively, to be compared with the

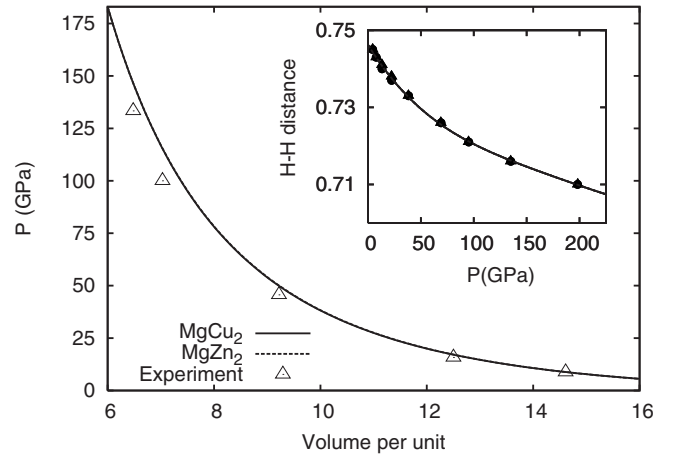


FIG. 2. Calculated zero-temperature equation of state of $\text{Ar}(\text{H}_2)_2$ in the MgCu_2 (solid line) and MgZn_2 (dashed line) crystal Laves structures. Experimental data is from work in Ref. 7. Inset: calculated pressure dependence of the H-H intermolecular distance in the MgCu_2 (solid line, solid dots) and MgZn_2 (dashed line, solid triangles) crystal structures. Volumes and distances are in units of $\text{\AA}^3/\text{particle}$ and \AA , respectively.

experimental values 8.77 and 15.79 GPa. It must be noted that the estimated equation of state and pressure dependence of the H-H intermolecular bond distance of the MgZn_2 and MgCu_2 phases appear to be indistinguishable within the numerical uncertainty in our calculations (namely, 1 GPa and 0.01 \AA , see Fig. 2).

Since hydrogen is a very light molecule, quantum zero-point motion corrections must be included in the calculations. Customarily this is achieved using quasiharmonic approaches that involve estimation of the vibrational phonon frequencies. In following this procedure, we found that $\text{Ar}(\text{H}_2)_2$ in the MgZn_2 structure always exhibits imaginary Γ -phonon frequencies at pressures below ~ 300 GPa. This means that the MgZn_2 structure is mechanically unstable, at least, at low temperatures. On the other hand, we found that the MgCu_2 structure is perfectly stable at all the studied pressures. Our numerical tests showed that this result does not depend on the approximation of the exchange-correlation functional used.¹⁸ In Fig. 3, we show the phonon frequency spectra of $\text{Ar}(\text{H}_2)_2$ in the MgCu_2 crystal structure calculated along a k -point path contained within the IBZ and at pressure ~ 200 GPa

Since the x-ray-resolved RT crystal structure of $\text{Ar}(\text{H}_2)_2$ is MgZn_2 ,³ we carried out a series of AIMD simulations of this and the MgCu_2 structure at $T = 300$ K in order to explore their stability. In fact, analysis of our simulations based on estimation of the averaged mean-squared displacement and position-correlation function¹⁹ showed that both MgCu_2 and MgZn_2 structures are mechanically stable at RT. On view of these results and the reported x-ray data, we concluded that a temperature-induced $\text{MgCu}_2 \rightarrow \text{MgZn}_2$ transition occurs at fixed P (or equivalently, a pressure-induced $\text{MgZn}_2 \rightarrow \text{MgCu}_2$ transition at fixed T , see Fig. 1). This temperature-induced transformation can be understood in terms of entropy: $\text{Ar}(\text{H}_2)_2$ in the MgZn_2 structure is highly anharmonic so ionic entropy contributions to the total free

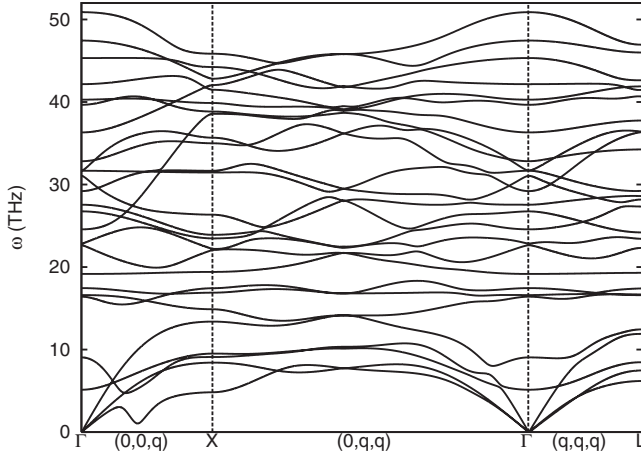


FIG. 3. Calculated phonon-frequency spectra of $\text{Ar}(\text{H}_2)_2$ in the MgCu_2 crystal structure at $V=5.83 \text{ \AA}^3/\text{particle}$ and $P\sim 200 \text{ GPa}$ (corresponding molecular vibron frequencies are not shown). The calculation was done on a supercell containing 16 Ar and 64 H atoms and using a $4\times 4\times 4$ k -point grid for IBZ sampling.

energy stabilize this structure over the MgCu_2 phase with raising temperature. In fact, IR measurements displayed a splitting of the vibron mode in the interval $35\leq T\leq 150 \text{ K}$.¹⁷ This splitting can be induced by the degeneracy removal of the infrared E_{1u} mode due to the decrease in the crystal quality caused by precursor effects of the $\text{MgZn}_2\rightarrow\text{MgCu}_2$ transition.

The causes of the aforementioned R-IR experimental disagreements can be rationalized in the light of the foreseen $\text{MgCu}_2\rightarrow\text{MgZn}_2$ transition, as we explain in what follows. In Fig. 4, we enclose the calculated R and IR vibron frequencies of $\text{Ar}(\text{H}_2)_2$ in the MgZn_2 , MgCu_2 , and AlB_2 structures as function of pressure. At high pressures, it is shown that the $A_{1g}(\text{R})$ vibron line corresponding to the MgZn_2 and MgCu_2 structures are practically identical, whereas they settle appreciably below the line estimated for the AlB_2 structure, and follow closely the low- T R results.³ These outcomes together with the energy and phonon results already presented, led us to think that the sudden disappearance of the R vibron mode observed at high P might be related to the $\text{MgCu}_2\rightarrow\text{MgZn}_2$ transition unraveled in this paper and not to pressure-induced metalliclike behavior³ or $\text{MgZn}_2\rightarrow\text{AlB}_2$ phase transition⁷ as previously suggested. In fact, accurate electronic density of states (DOS) analysis performed on the perfect MgZn_2 , MgCu_2 , and AlB_2 crystal structures show no closure of the electronic band gap up to compressions of at least 420 GPa. Furthermore, the $E_{1u}(\text{IR})$ vibron line that we calculated for the MgZn_2 structure (see Fig. 4) agrees closely with Datchi's IR data obtained at high pressures. This accordance is coherent if one considers that the series of IR experiments were realized near the edge of the MgCu_2 - MgZn_2 phase boundary, as we sketch in Fig. 1. Conclusive experiments confirming the validity of our statements might consist of new series of x-ray and IR measurements performed at temperatures below 100 K and high pressures; according to our predictions, the vibron signature will eventually disappear at the crossing with the MgCu_2 - MgZn_2 phase boundary since IR vibron modes in the MgCu_2 structure are inactive.

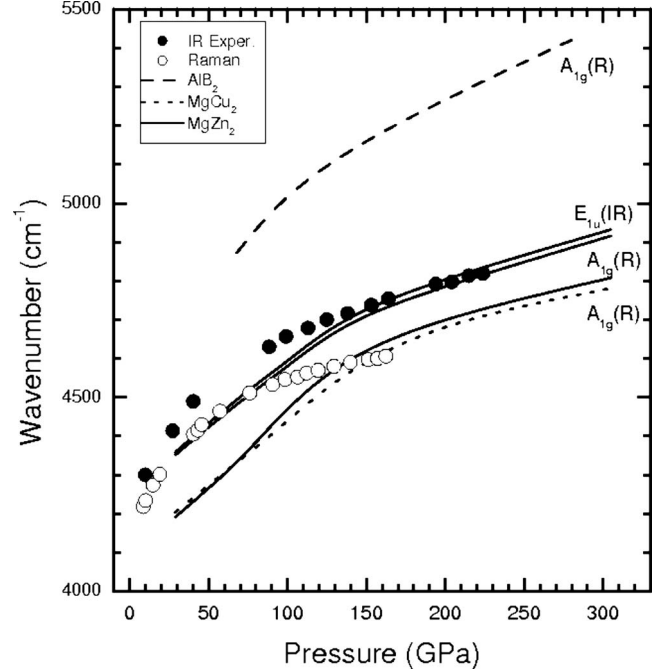


FIG. 4. Calculated R and IR vibron lines of $\text{Ar}(\text{H}_2)_2$ in the MgZn_2 , MgCu_2 , and AlB_2 structures as function of pressure. Experimental data from Ref. 3 (\circ) and Ref. 6 (\bullet) are shown.

B. High- T results

An intriguing physical phenomenon has been recently predicted and subsequently observed in H_2 under pressure. It consists in the appearance of a maximum peak on its melting line followed by a negative $\partial T_m/\partial P$ slope.^{20,21} This phenomenon have been explained in terms of subtle changes on the intermolecular forces due to compression instead of more familiar arguments like promotion of valence electrons to higher energy orbitals or occurrence of molecular dissociation processes. Motivated by these interesting findings on hydrogen, we investigated the dynamical properties of $\text{Ar}(\text{H}_2)_2$ at high P and high T in the search of similar physical manifestations and to provide further understanding of vdW compounds in general. There exist several well-established techniques by which one can determine the melting line of a material; these essentially base on solid-liquid phase coexistence simulations and/or Gibbs free-energy calculations.²² Application of these methods at quantum first-principles level of description, however, turns out to be computationally very intensive and laborious. A simulation approach that has proved successful in reproducing general melting trends in materials at affordable computational cost, including experimental negative melting slopes, is the ‘‘heat-until-it-melts’’ method.^{23,24} This technique allows for estimation of a precise upper bound of the solid-liquid phase boundary of interest. It must be stressed that we did not pursue accurate calculation of the melting line of $\text{Ar}(\text{H}_2)_2$ but to identify possible anomalous effects on it.

Results from our AIMD simulations are shown in Fig. 5 and can be summarized as follows: (i) the lattice of H_2 molecules melts at temperatures significantly lower than the whole crystal does so leading to mixtures of liquid H_2 and

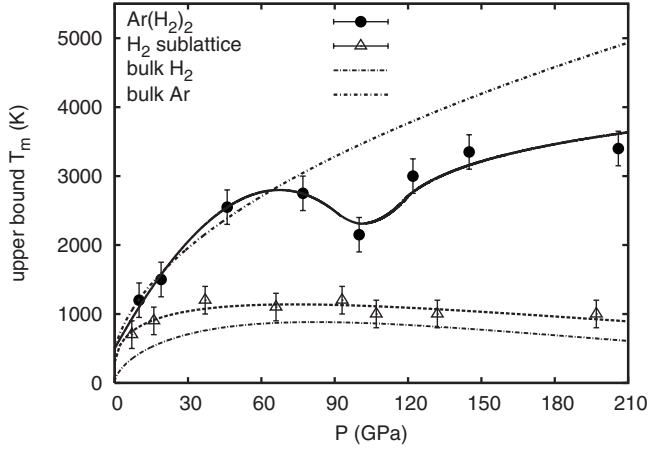


FIG. 5. Upper bound of the melting line of $\text{Ar}(\text{H}_2)_2$ under pressure (solid line). Melting states obtained in the AIMD simulations are indicated with \bullet and corresponding error bars amount to 200 K. Thermodynamic states at which the lattice of hydrogen molecules is observed to melt in the simulations are represented by \triangle (fitted to a dashed line). The melting line of pure Ar (Ref. 25) (long-dashed and dotted line) and H_2 (Ref. 20) (dashed and dotted line) are shown for comparison.

solid Ar over wide P - T ranges; (ii) the fusion of the H_2 lattice occurs at temperatures very close to the melting line of pure hydrogen while $\text{Ar}(\text{H}_2)_2$ as a whole practically reproduces the melting behavior of pure Ar up to ~ 60 GPa; and (iii) the value of the estimated $\partial T_m / \partial P$ slope is negative within the pressure interval $60 \leq P \leq 110$ GPa whereas positive elsewhere. Results (i) and (ii) can be interpreted in terms of similar arguments than recently disclosed in solid mixtures of Ne-He and Ar-He, namely: lattices composed of same-species particles effectively behave like not interacting one with another but following alike physical trends (bond distance, compressibility, etc.) than found in their respective pure system.¹¹ In fact, we recently conjectured the superior energy stability of the MgCu_2 structure over MgZn_2 in $\text{Ar}(\text{H}_2)_2$, as rigorously demonstrated here, using this type of reasoning and crystal-symmetry arguments.¹¹ Regarding result (iii), this is in itself a manifestation of a very peculiar and intriguing physical phenomenon. In general, systems presenting negative melting slope are characterized by open crystalline structure (water and graphite), surpassing promotion of valence electrons in the fluid phase (alkali metals) or continuous changing interparticle interactions (molecular hydrogen). In the present case either open crystalline structure or electronic band promotion effects (energetically prohibitive) can be ruled out, so changes in the interparticle interactions holds as the likely cause. The question to be answered next then is: what is the exact nature of these changing interactions, or more precisely, do they relate to dramatic changes in electronic structure, are the ionic degrees of freedom and effective decoupling of the Ar and H_2 lattices crucial to them? In order to detect possible electronic phase transitions and/or molecular-dissociation processes, we performed meticulous averaged DOS and H-H radial correlation function ($g_{\text{H-H}}$) analysis over the atomic configurations generated in the AIMD runs. Within the thermodynamic

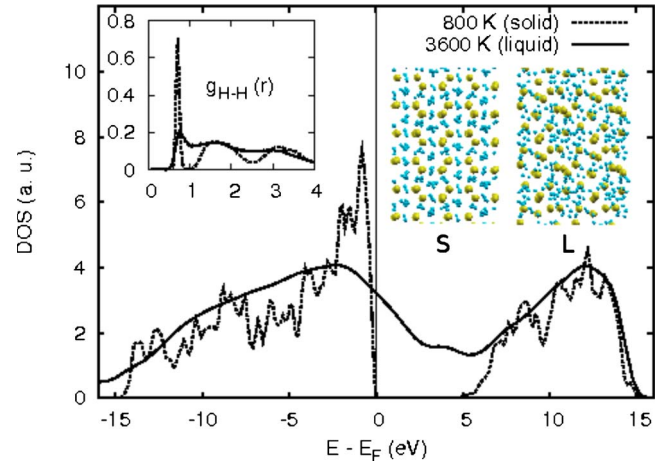


FIG. 6. (Color online) DOS of $\text{Ar}(\text{H}_2)_2$ calculated at $P \sim 210$ GPa ($V = 5.83 \text{ \AA}^3/\text{particle}$) and different temperatures. Inset: Averaged radial H-H pair distribution function $g_{\text{H-H}}$ obtained for the liquid (solid line) and solid (dashed line) phases (distance is in units of \AA). Snapshots of liquid (L) and solid (S) configurations as generated in the AIMD simulations; dissociated H_2 molecules are observed in L.

range $60 \leq P \leq 110$ GPa and $0 \leq T \leq 3500$ K (where $\partial T_m / \partial P \leq 0$), we found that $\text{Ar}(\text{H}_2)_2$ is always an insulator material, either solid or liquid, where H_2 molecules remain stable. Therefore, dramatic changes in electronic structure can be discarded as the originating mechanism behind the alternating sign of $\partial T_m / \partial P$. Actually, on the contrary case, one would have expected the value of $\partial T_m / \partial P$ to be negative also beyond ~ 110 GPa since, in principle, there is not reason to think that the originating electronic effects go missing at higher P . Interestingly, at compressions above ~ 210 GPa and temperatures high enough for the system to melt we did observe closure of the electronic energy band gap; according to $g_{\text{H-H}}$ analysis and visual recreation of the AIMD configurations, this electronic phase transition is a consequence of emergent H_2 dissociation processes. In Fig. 6, we enclose DOS and $g_{\text{H-H}}$ results that illustrate this insulator-to-metal phase transition. It is worth noticing that this result is consistent with shock-wave compression experiments²⁶ and *ab initio* investigations²⁰ performed on pure hydrogen. With regard to the predicted negative melting slope, ionic effects are the likely subjacent cause. Considering results (i) and (ii) above, one can envisage a plausible explanation of this phenomenon: since the lattice of H_2 molecules melts at temperatures much lower than the lattice of Ar atoms does, collisions between diffusive H_2 molecules and localized Ar atoms act like effective thermal-like excitations on the last that ultimately provoke the global melting of the system at temperatures below those of pure Ar. H_2 itself presents negative melting slope beyond ~ 60 GPa so this effect is echoed and enhanced substantially, in the melting line of $\text{Ar}(\text{H}_2)_2$ (see Fig. 5). Beyond ~ 110 GPa, the stability of the Ar lattice becomes further reinforced so the effect of H_2 collisions there is just to deplete the slope of the global melting curve in comparison to that of pure Ar. In order to test the validity of such hypothesis, we performed a series of AIMD simulations at $P \sim 110$ GPa ($V = 7.50 \text{ \AA}^3/\text{particle}$) in which we

kept the lattice of H₂ molecules *frozen* and left the lattice of Ar atoms to evolve. Under these conditions we found that fusion of the Ar structure occurs at temperatures ~ 900 K above that of pure Ar, hence the original melting mechanism proposed seems to be corroborated. Analogous melting behavior than described here can be expected in other rare-gas H₂ compounds, such as Xe(H₂)₇, and maybe also in SiH₄(H₂)₂ and CH₄(H₂).

IV. CONCLUDING REMARKS

To summarize, we have studied the behavior of Ar(H₂)₂ under pressure at low and high temperatures using computational first-principles techniques. As results, we have unraveled (i) temperature(pressure)-induced solid-solid phase tran-

sitions that may resolve the existing discrepancies between the sets of R and IR experimental data and (ii) an anomalous melting phenomenon consisting of negative melting slope. The atypical melting line of Ar(H₂)₂ can be understood in terms of the decoupling of H₂ and Ar ionic degrees of freedom and of coexistence of same-species liquid and solid phases. Metallization of liquid Ar(H₂)₂ is predicted at high P - T conditions.

ACKNOWLEDGMENTS

D.E. acknowledges support of MICINN of Spain (Grants No. CSD2007-00045 and No. MAT2007-65990-C03-01). The authors acknowledge computational resources on the U.K. National Supercomputing HECToR service.

*c.silva@ucl.ac.uk

- ¹M. Stadele and R. M. Martin, Phys. Rev. Lett. **84**, 6070 (2000); P. Loubeyre, F. Occelli, and R. Letoullec, Nature (London) **416**, 613 (2002).
- ²C. Narayana, H. Luo, H. Orloff, and A. L. Ruoff, Nature (London) **393**, 46 (1998).
- ³P. Loubeyre, R. Letoullec, and J.-P. Pinceaux, Phys. Rev. Lett. **72**, 1360 (1994).
- ⁴T. A. Strobel, M. Somayazulu, and R. J. Hemley, Phys. Rev. Lett. **103**, 065701 (2009).
- ⁵E. Zurek, R. Hoffmann, N. W. Ashcroft, A. R. Oganov, and A. O. Lyakhov, Proc. Natl. Acad. Sci. U.S.A. **106**, 17640 (2009).
- ⁶F. Datchi, P. Loubeyre, R. Letoullec, A. F. Goncharov, R. J. Hemley, and H. K. Mao, Bull. Am. Phys. Soc. **41**, 564 (1996).
- ⁷S. Bernard, P. Loubeyre, and G. Zerah, Europhys. Lett. **37**, 477 (1997).
- ⁸N. Matsumoto and H. Nagara, J. Phys.: Condens. Matter **19**, 365237 (2007).
- ⁹M. Somayazulu, P. Dera, A. F. Goncharov, S. A. Gramsch, P. Liermann, W. Yang, Z. Liu, H.-k. Mao, and R. J. Hemley, Nat. Chem. **2**, 50 (2010).
- ¹⁰H. Chacham and B. Koiller, Phys. Rev. B **52**, 6147 (1995).
- ¹¹C. Cazorla, D. Errandonea, and E. Sola, Phys. Rev. B **80**, 064105 (2009).
- ¹²G. Kresse and J. Furthmuller, Phys. Rev. B **54**, 11169 (1996); Y. Wang and J. P. Perdew, *ibid.* **44**, 13298 (1991).
- ¹³H. J. Monkhorst and J. D. Pack, Phys. Rev. B **13**, 5188 (1976).
- ¹⁴G. Kresse, J. Furthmuller, and J. Hafner, Europhys. Lett. **32**, 729 (1995).
- ¹⁵D. Alfe, Comput. Phys. Commun. **180**, 2622 (2009).
- ¹⁶H. Fukui, N. Hirao, Y. Ohishi, and A. Q. R. Baron, J. Phys.: Condens. Matter **22**, 095401 (2010).
- ¹⁷L. Ulivi, R. Bini, P. Loubeyre, R. Le Toullec, and H. J. Jodl, Phys. Rev. B **60**, 6502 (1999).
- ¹⁸D. M. Ceperley and B. J. Alder, Phys. Rev. Lett. **45**, 566 (1980).
- ¹⁹L. Vocadlo, D. Alfe, M. J. Gillan, I. G. Wood, J. P. Brodholt, and G. D. Price, Nature (London) **424**, 536 (2003).
- ²⁰S. A. Bonev, E. Schwegler, T. Ogitsu, and G. Galli, Nature (London) **431**, 669 (2004).
- ²¹S. Deemyad and I. F. Silvera, Phys. Rev. Lett. **100**, 155701 (2008).
- ²²M. J. Gillan, D. Alfe, J. Brodholt, L. Vocadlo, and G. D. Price, Rep. Prog. Phys. **69**, 2365 (2006); D. Alfe, M. J. Gillan, and G. D. Price, Nature (London) **401**, 462 (1999).
- ²³I. Tamblyn, J.-Y. Raty, and S. A. Bonev, Phys. Rev. Lett. **101**, 075703 (2008).
- ²⁴J.-Y. Raty, E. Schwegler, and S. A. Bonev, Nature (London) **449**, 448 (2007).
- ²⁵E. Pechenik, I. Kelson, and G. Makov, Phys. Rev. B **78**, 134109 (2008).
- ²⁶S. T. Weir, A. C. Mitchell, and W. J. Nellis, Phys. Rev. Lett. **76**, 1860 (1996).